Synchronized Chaos and Other Coherent States for two Coupled Neurons *

Frank Pasemann
Max-Planck-Institute for Mathematics in the Sciences
D-04103 Leipzig, Germany
email: f.pasemann@mis.mpg.de

Abstract

The parametrized time-discrete dynamics of two recurrently coupled chaotic neurons is investigated. Basic dynamical features of this system are demonstrated for symmetric couplings of identical neurons. Periodic as well as chaotic orbits constrained to a manifold M of synchronized states are observed. Parameter domains for locally stable synchronization manifolds M are determined by numerical simulations. In addition to the synchronized dynamics there often co-exist periodic, quasiperiodic and even chaotic attractors representing different kinds of non-synchronous coherent dynamics. Simulation results for selected sets of parameters are presented, and synchronization conditions for systems with non-identical neurons are derived. Also these more general systems inherit the above mentioned dynamical properties.

*MIS-MPG Preprint 44/98, and *Physica D*, **128**, 236–249, (1999).

1 Introduction

In many recent articles the feasibility of synchronizing chaotic systems has been investigated experimentally as well as theoretically [4], [7], [11], [12], [15], [17], [23], [24], [26], [29], [31]. Interest in the construction of chaotic synchronized dynamical systems has aroused mainly because of its potential for application in secure communication [2], [5], [16], [18], [20]. Most of the work therefore investigates the coupling of time-continuous systems like Lorenz or Rössler systems, or like Chua's circuit. But also time discrete systems are considered [6]. Synchronization in coupled systems can be achieved in different ways: by one-way couplings as introduced in [23], or by recurrent couplings, where each of the systems effects the other [11]. In this paper we discuss the discrete-time dynamics of two 1-dimensional chaotic systems coupled recurrently. The corresponding maps are considered to represent a simple model of formal neurons [21].

We will use the term "synchronization" in the sense of *complete synchronization* of chaotic systems; i.e. we consider systems, the states of which can coincide, while the dynamics in time remains chaotic [27]. We may also discern between global and local synchronization. Global synchronization means, that for almost all initial conditions orbits of the systems will synchronize. By local synchronization we refer to locally stable synchronized states; i.e. small perturbations will not desynchronize the systems. We will also make use of the concept of a synchronization manifold [11] to which a synchronized dynamics is constrained.

Besides the discussion of synchronized chaos in the context of technical applications, selective synchronization of neural activity in biological brains was often suggested to be a fundamental temporal mechanism for binding spatially distributed features into coherent objects. (cf. among many others [8], [9], [30]). Motivated by these biological findings synchronization of chaos has been studied in computer simulations for networks with spiking neurons, and in large networks of Hindmarsh-Rose neurons [3], [10], [25]. With respect to discrete-time dynamics conditions for synchronized chaos were discussed also for large networks consisting of coupled pools of analog neurons [32].

On this background we were interested in the discrete dynamics of two coupled chaotic neuromodules that exhibit complete synchronization. Simulation results for synchronization and other coherent states in coupled chaotic modules of two coupled chaotic standard analog neurons were presented in [22]. But here we show that already for a system composed of two interacting chaotic neurons – i.e. standard neurons with a damping term [21] – we observe global as well as local synchronization of chaotic dynamics. Interesting parameters are the stationary inputs to neurons as well as the strength of the recurrent couplings. The corresponding dynamics is analyzed in section 3 for the case of symmetrically coupled identical neurons. Numerical simulations reveal that for large parameter domains various non-synchronous periodic, quasiperiodic or even chaotic attractors may co-exist with a synchronized dynamics. Orbits in the synchronization manifold

may be locally stable or unstable. The instability of synchronized chaotic orbits is signaled by two positive Lyapunov exponents indicating hyperchaos [14], [28]. Hyperchaos as a signal for the transition from synchronized to non-synchronized states in the chaotic regime was also observed in [6].

Most of these dynamical phenomena are also found for the more general case of recurrently coupled non-identical chaotic neurons. Conditions on the coupling strength are derived for the existence of synchronized dynamics in this case, and in section 4 corresponding simulation results are shortly discussed.

2 Two coupled chaotic neurons

The simplest example of two coupled neuromodules is the case where each module consists only of one single neuron. The parametrized discrete activity dynamics of a single chaotic neuron is given by the 1-dimensional map (1), which is bimodal for a large class of parameter values, and thus has parameter domains where chaotic attractors exist [21]. Therefore, synchronized chaotic dynamics for specific recurrent couplings of two "chaotic" neurons, A and B say, has to be expected. This is the situation we analyze in the following.

The discrete activity dynamics of a single chaotic neuron A is given by

$$a(t+1) = \theta^A + \gamma^A \cdot a(t) + w^A \cdot \sigma(a(t)) \ , \quad , \quad a \in \mathbf{R} \quad , \quad 0 \leq \gamma < 1 \ , \qquad (1)$$

and for unit B with activity b correspondingly. Here γ^A denotes the damping term, w^A the self-coupling of neuron A; $\theta^A := (\theta_0^A + I^A)$ describes the sum of a fixed bias term θ_0^A of A and its stationary external input I^A. The output $o^A = \sigma(a)$ is given by the sigmoidal transfer function

$$\sigma(a) := \frac{1}{1+e^{-a}} \quad . \qquad (2)$$

By $\rho^A := (\gamma^A,\ \theta^A,\ w^A)$ we denote the set of parameters for the single unit dynamics.

If we couple the neurons by connections w^{AB} and w^{BA}, respectively, and denote the set of parameters for the coupled system by $\rho := (\rho^A,\ \rho^B,\ w^{AB},\ w^{BA})$ the corresponding dynamics $F_\rho : \mathbf{R}^2 \to \mathbf{R}^2$ reads

$$\begin{aligned} a(t+1) &= \theta^A + \gamma^A \cdot a(t) + w^A \cdot \sigma(a(t)) + w^{AB} \cdot \sigma(b(t)) \ , \\ b(t+1) &= \theta^B + \gamma^B \cdot b(t) + w^B \cdot \sigma(b(t)) + w^{BA} \cdot \sigma(a(t)) \ . \end{aligned} \qquad (3)$$

In the following we are interested especially in the process of *complete synchronization* of neurons, which in this case means that there exists a subset $D \subset \mathbf{R}^2$ such that $(a_0, b_0) \in D$ implies

$$\lim_{t\to\infty} \mid a(t;a_0) - b(t;b_0) \mid = 0 \ ,$$

where $(a(t;a_0), b(t;b_0))$ denotes the orbit under F_ρ through the initial condition (a_0, b_0). The synchronization is called *global* if $D \equiv \mathbf{R}^2$, and *local* if $D \subset \mathbf{R}^2$ is a proper subset. Thus, a *synchronized state* s of the coupled system is defined by $s := a = b$. Correspondingly, a state $\hat{s}$ satisfying $\hat{s} = a = -b$ is called *anti-synchronized*. Here, the *synchronization manifold* $M := \{(s,s) \in \mathbf{R}^2 \mid s = a = b\}$ of synchronized states corresponds to a 1-dimensional hyperplane $M \cong \mathbf{R} \subset \mathbf{R}^2$. We introduce coordinates parallel and orthogonal to the synchronization manifold M [11] as follows:

$$\xi := \frac{1}{\sqrt{2}}(a+b) \quad , \quad \eta := \frac{1}{\sqrt{2}}(a-b) \; . \tag{4}$$

But setting $a - b = 0$ we can immediately read from equation (3) the following

Lemma 1 *Let the parameter sets ρ^A, ρ^B of the units A and B satisfy*

$$\gamma = \gamma^A = \gamma^B \; , \quad \theta = \theta^A = \theta^B \; , \quad (w^A - w^{BA}) = (w^B - w^{AB}) \; . \tag{5}$$

Then every orbit of $\tilde{F}_\rho$ through a synchronized state $s \in M$ is constrained to M for all times.

Especially, lemma 1 applies to the case of identical neurons with symmetric couplings, i.e. to a $\rho = (\gamma, \theta, w, w^{coup})$ with

$$\gamma = \gamma^A = \gamma^B \; , \quad \theta = \theta^A = \theta^B \; , \quad w = w^A = w^B \; , \quad w^{coup} = w^{BA} = w^{AB} \; . \tag{6}$$

We will consider the special parameter setting (6) first.

3 Coupling two identical neurons

Let $\rho = (\gamma, \theta, w, w^{coup})$ denote a parameter set (6) of two coupled identical neurons. We will fix the damping term $\gamma = 0.6$ and the self-connection $w = -16.0$ so that the chaotic domain for the single neuron can be reached [21]. Changing now to (ξ, η)-coordinates given by (4) and setting

$$w^+ := (w + w^{coup}) \quad , \quad w^- := (w - w^{coup}) \; , \tag{7}$$

we obtain the dynamics $\tilde{F}_\rho$ of two coupled identical neurons as

$$\begin{aligned} \xi(t+1) &= \gamma \cdot \xi(t) + \sqrt{2} \cdot \theta + \frac{w^+}{\sqrt{2}} \cdot G^+(\xi(t), \eta(t)) \; , \\ \eta(t+1) &= \gamma \cdot \eta(t) + \frac{w^-}{\sqrt{2}} \cdot G^-(\xi(t), \eta(t)) \; , \end{aligned} \tag{8}$$

where the functions G^+, $G^- : \mathbf{R}^2 \to \mathbf{R}$ are defined by

$$G^+(\xi,\eta) := \sigma(\frac{1}{\sqrt{2}}(\xi+\eta) + \sigma(\frac{1}{\sqrt{2}}(\xi-\eta)) \; ,$$
$$G^-(\xi,\eta) := \sigma(\frac{1}{\sqrt{2}}(\xi+\eta) - \sigma(\frac{1}{\sqrt{2}}(\xi-\eta)) \; . \tag{9}$$

According to lemma 1 every orbit of $\tilde{F}_\rho$ through a synchronized state $(\xi,0) \in M$ is constrained to M for all times. With $s := 1/\sqrt{2}\,\xi$, the corresponding synchronized 1-dimensional dynamics F^s_ρ in M is described by the equation

$$s(t+1) = \theta + \gamma \cdot s(t) + w^+ \cdot \sigma(s(t)) \; . \tag{10}$$

Thus, the synchronized dynamics F^s_ρ comprises the whole spectrum of dynamical behavior of a single isolated chaotic neuron [21] with self-connection w^+; i.e. it may have fixed point attractors as well as periodic or chaotic ones. Although the persistence of synchronized dynamics for identical neurons is guaranteed by condition (6), it is not at all clear that the synchronization manifold M is itself asymptotically stable with respect to the dynamics $\tilde{F}_\rho$. Thus, an $\tilde{F}_\rho$-invariant set $\mathcal{A} \subset M$ may be an attractor for the synchronized dynamics F^s_ρ but not for the dynamics $\tilde{F}_\rho$ of the coupled system. The simulation results in the next section will give a first idea about the dynamical complexity of this "trivial" neural system.

But first let us introduce the point-reflection operator $\mathbf{S}^\eta$ acting only on the η-coordinates of the (ξ,η)-phase space, i.e.

$$\mathbf{S}^\eta(\xi,\eta) = (\xi,-\eta) \; .$$

The functions G^+ and G^- defined in (9) have the property

$$G^+ \; \mathbf{S}^\eta(\xi,\eta) = G^+(\xi,\eta) \quad , \quad G^- \; \mathbf{S}^\eta(\xi,\eta) = -G^-(\xi,\eta) \; .$$

Thus the dynamics $\tilde{F}_\rho : \mathbf{R}^2 \to \mathbf{R}^2$ given by equation (8) is equivariant under the action of $\mathbf{S}^\eta$; i.e.

$$\tilde{F}_\rho \, (\xi,\eta) = (\mathbf{S}^\eta)^{-1} \, \tilde{F}_\rho \, \mathbf{S}^\eta(\xi,\eta) \; .$$

As a consequence of this equivariance property we obtain the following

Lemma 2 *Let $\tilde{F}_\rho$ denote the dynamics (8) of two coupled identical neurons, and let F^p_ρ denote its p-fold iterate. For a point $(\xi,\eta) \in \mathbf{R}^2$ we then have*

$$(\xi,\eta) = \tilde{F}^p_\rho \, (\xi,\eta) \quad \Longleftrightarrow \quad (\xi,-\eta) = \tilde{F}^p_\rho \, (\xi,-\eta) \; .$$

The fact that with (ξ,η) also $(\xi,-\eta)$ must be a p-periodic point does of course *not* include that both points belong to the same p-periodic orbit. An example can be found for $\rho = (0.6, 3.75, -16.0, 2.0)$, where two period-7 attractors are interwoven. As a trivial consequence of lemma 2 we have

Corollary 1 *Let $\tilde{F}_\rho$ denote the dynamics of two coupled identical neurons. If (ξ, η) and $(\xi, -\eta)$ belong to the same period-p orbit of $\tilde{F}_\rho$ then $p = 2q$, and $(\xi, -\eta) = \tilde{F}_\rho^q(\xi, \eta)$.*

For the description of attractors observed for the dynamics of coupled chaotic neurons we will use the following definition: A quasiperiodic or chaotic attractor is called *p-cyclic* if it has p connected components which are permuted cyclically by the map $\tilde{F}_\rho$. Every component of a p-cyclic attractor is an attractor of $\tilde{F}_\rho^p$.

To discuss the qualitative aspects of the dynamics $\tilde{F}_\rho$ for the identical coupled chaotic neurons we make use of the following Lyapunov exponents. Exponents (λ_1, λ_2) are derived from the linearization of F_ρ (3); i.e. from

$$DF_\rho(a(t), b(t)) = \begin{pmatrix} \gamma + w \cdot \sigma'(a(t)) & w^{coup}\sigma'(b(t)) \\ w^{coup}\sigma'(a(t)) & \gamma + w \cdot \sigma'(b(t)) \end{pmatrix} . \tag{11}$$

For the synchronized dynamics the *synchronization exponent* λ^s and the *transversal exponent* $\lambda^\perp$ are derived from the linearization of $\tilde{F}_\rho$ (8) around synchronized states $s(t) = \frac{1}{\sqrt{2}} \cdot \xi(t)$. With

$$D\tilde{F}_\rho(s) = \begin{pmatrix} \epsilon^s(s) & 0 \\ 0 & \epsilon^\perp(s) \end{pmatrix} := \begin{pmatrix} \gamma + w^+ \cdot \sigma'(s) & 0 \\ 0 & \gamma + w^- \cdot \sigma'(s) \end{pmatrix} \tag{12}$$

we have

$$\lambda^s = \lim_{n\to\infty} \frac{1}{n} \sum_{t=1}^{n} ln\,|\,\epsilon^s(s(t))| \quad , \quad \lambda^\perp = \lim_{n\to\infty} \frac{1}{n} \sum_{t=1}^{n} ln\,|\,\epsilon^\perp(s(t))| \quad . \tag{13}$$

3.1 Results from numerical simulations

To get an idea about what kind of synchronized dynamics does exist for coupled neurons and for what parameter values it is locally stable or unstable we discuss results presented in figures 1 and 2. In figure 1 the Lyapunov exponents λ^s and $\lambda^\perp$ are displayed in dependence of the coupling strength w^{coup} for $\gamma = 0.6$, $w = -16$, and $\theta = 4.0$. The corresponding bifurcation diagram for the synchronized dynamics F_ρ^s given by equation (10) is also shown. We observe a standard period-doubling route to chaos, and for a large domain of coupling strengths, i.e. $-5.74 < w^{coup} < 1.89$, there exist chaotic orbits in the synchronization manifold M.

Furthermore, for $w^{coup} < 0$ there is a domain where both Lyapunov exponents λ^s, $\lambda^\perp$ are positive. This hyperchaotic domain signals of course the instability of synchronized states. Reading from the data underlying figure 1 hyperchaos appears in the interval $-3.51 < w^{coup} < 0$; i.e. for couplings from this interval there exist no locally stable synchronized chaotic orbits. In fact, as is shown in figure 4 for $w^{coup} = -3$, the attractors of the coupled system are not constrained to the synchronization manifold M. But there is also a coupling domain $-5.74 < w^{coup} < -3.51$ where we have a (locally) stable synchronized chaotic

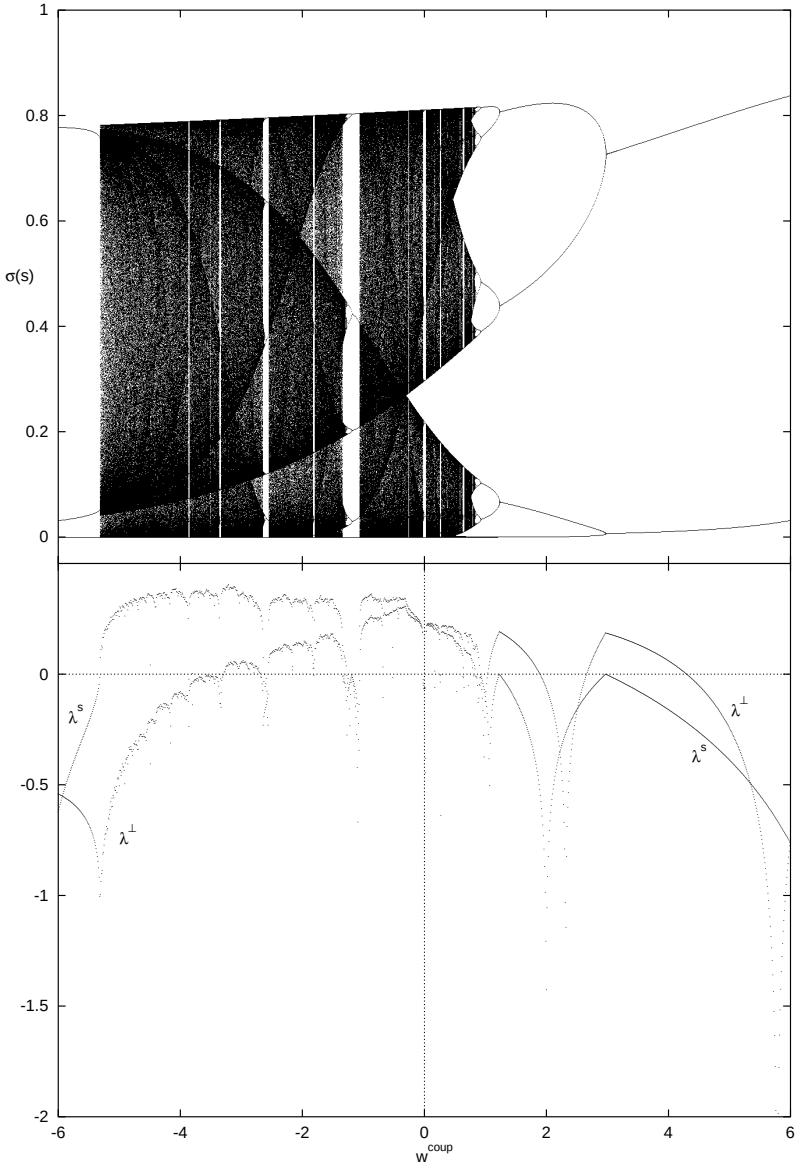

Figure 1: Bifurcation diagram for the synchronized dynamics $s(t)$ with respect to parameter w^{coup}; other parameters are $\gamma = 0.6$, $w = -16$, and $\theta = 4$. Below synchronization (λ^s) and transversal ($\lambda^\perp$) Lyapunov exponents are plotted for the same w^{coup}-interval. A positive λ^s indicates a synchronized chaotic attractor, a positive $\lambda^\perp$ indicates an unstable synchronization manifold M.

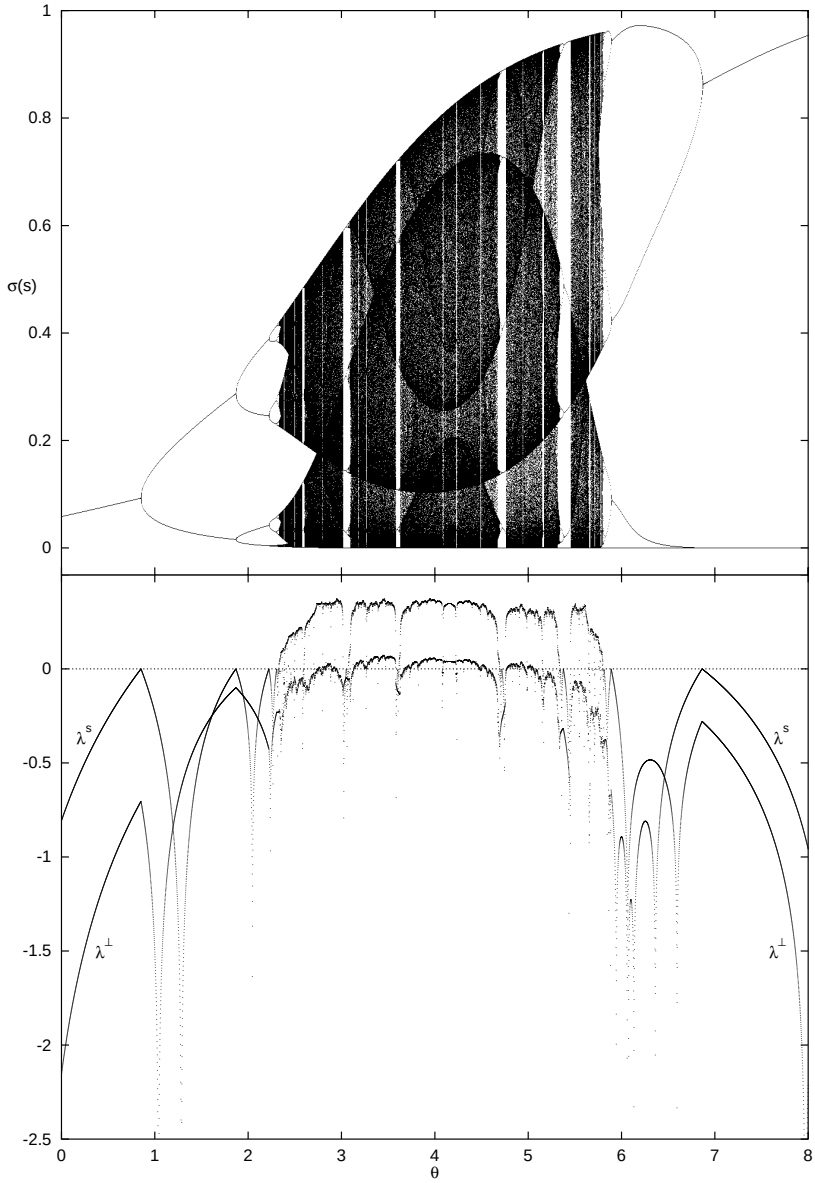

Figure 2: Bifurcation diagram for the synchronized dynamics $s(t)$ with respect to parameter θ; other parameters are $\gamma = 0.6$, $w = -16$, and $w^{coup} = -3.0$. Below synchronization (λ^s) and transversal ($\lambda^\perp$) Lyapunov exponents are plotted for the same θ-interval. A positive λ^s indicates a synchronized chaotic attractor, a positive $\lambda^\perp$ indicates an unstable synchronization manifold M.

dynamics; i.e. where $\lambda^s > 0$ and $\lambda^\perp < 0$. In general, these chaotic attractors constrained to M co-exist with other periodic or quasiperiodic attractors arranged symmetrically around M. An example of this dynamic configuration is presented in figure 3 where a synchronized chaotic attractor co-exists with a period-2 and a period-4 attractor. Outside the interval $-22.6 < w^{coup} < -5.74$ we find only globally stable synchronized periodic and chaotic attractors. For $w^{coup} < -22.6$ the synchronization manifold M becomes unstable again and the dynamic situation is characterized by two or more (chaotic) attractors again arrange symmetrically to M.

Also for positive couplings hyperchaos is observed. This is the case, for instance, in the interval $0 < w^{coup} < 0.90$. But here the transversal exponent $\lambda^\perp$ is larger then the synchronization exponent λ^s. Again, there is no locally stable synchronized dynamics for these values of w^{coup}. Typically, there exists a local hyperchaotic attractor traversing the unstable synchronization manifold M; figure 7 shows a characteristic situation. Again, these chaotic attractors often co-exist with periodic, quasiperiodic or other chaotic attractors. For $0.9 < w^{coup}$ we observe intervals, i.e. $1.03 < w^{coup} < 1.89$ and $2.66 < w^{coup} < 4.29$, where $\lambda^\perp > 0$ although $\lambda^s < 0$. This indicates the instability of the synchronization manifold M and of the periodic orbits constrained to it. Figure 8 displays the situation shortly after the synchronized period-4 orbit became locally stable. For $4.29 < w^{coup} < 6.24$ a locally stable synchronized period-2 attractor co-exists with an anti-synchronized one. The latter survives in the interval $6.24 < w^{coup} < 13.37$ as a global attractor (unstable M!) "jumping" to a synchronized global fixed point attractor after crossing a hysteresis interval $12.91 < w^{coup} < 13.37$.

Figure 2 displays the bifurcation diagram for the synchronized dynamics $s(t)$ with respect to the parameter θ; fixed parameters are $\gamma = 0.6$, $w = -16$, and $w^{coup} = -3.0$. The synchronized dynamics again follows period doubling bifurcations to chaos. For the same θ-range the Lyapunov exponents λ^s and $\lambda^\perp$ are displayed in figure 2. The data underlying this figure reveal that synchronized chaotic orbits ($\lambda^s > 0$) exist in the interval $2.33 < \theta < 5.8$. Included in this interval is a hyperchaotic θ-domain where in addition to $\lambda^s > 0$ also the transversal exponent $\lambda^\perp$ is positive; this interval is given by $2.74 < \theta < 5.05$. For θ outside of this interval the synchronization manifold M together with the periodic orbits constrained to M will be (locally) stable.

From the figures 1 and 2 we can deduce that for inhibitory couplings $w^{coup} < 0$ and positive synchronization exponents $\lambda^s > 0$ we have $\lambda^\perp < \lambda^s$. From the defining equations (13) this can be seen as follows: With $w < w^{coup} < 0$ for the eigenvalues ϵ^s and $\epsilon^\perp$ we have

$$\gamma - \frac{|w| + |w^{coup}|}{4} < \epsilon^s(s) < \gamma \quad , \quad \gamma - \frac{|w| - |w^{coup}|}{4} < \epsilon^\perp(s) < \gamma \quad , \quad s \in \mathbf{R} \, .$$

Because $\sigma'(0) = 0.25$, the left hand side of the inequalities correspond to $\epsilon^s(0)$ and $\epsilon^\perp(0)$. Therefore, states $s(t)$ on a synchronized chaotic orbit ($\lambda^s > 0$) must

visit the vicinity of the origin very often; i.e. for these states $|\epsilon^s(s)| > 1$, or, deduced from the above inequalities, $\epsilon^s(s) < -1$. But we have $\epsilon^\perp(s) = \epsilon^s(s) + 2 \cdot |w^{coup}|\sigma'(s) < \gamma < 1$ so that $|\epsilon^\perp(s)| < |\epsilon^s(s)|$ for states s satisfying $\sigma'(s) < \frac{(1+\gamma)}{|w^+|}$. But we then have: If $\lambda^s > 0$ then $\lambda^\perp < \lambda^s$. A corresponding argument holds for excitatory couplings $w^{coup} > 0$: If $\lambda^\perp > 0$ then $\lambda^s < \lambda^\perp$.

Finally we want to point out that outside of the synchronization manifold M we can observe bifurcation sequences to chaos which do not follow the usual period-doubling route. Reading in the direction of decreasing θ-values, here chaos appears after a transition from period-4 attractors to quasiperiodic attractors to chaotic ones to hyperchaotic ones. This type of sequence can be observed, for instance, for parameters $\gamma = 0.6$, $w = -16$, $w^{coup} = -2.0$ in the interval $4.2 < \theta < 4.7$. The whole scenario resembles the one called *chaotic contact bifurcation* (CCB) in [1]. Since M is unstable in this region, these 4-cyclic attractors are symmetric to M.

With respect to the dynamics $\tilde{F}_\rho$ given by equation (3), in the following we will describe the dynamical situation displayed in figures 3 to 8. They correspond to the six parameter sets listed in table 1.

Corresponding to Lemma 2, for ρ_1 we observe one period-2 and one period-4 attractor arranged symmetrically around the synchronization manifold M. They co-exist with a chaotic attractor ($\lambda^s = 0.35,\ \lambda^\perp = -0.07$) constrained to M. Here $\lambda^\perp < 0$ indicates that the synchronization manifold M is stable (compare figure 3 and table 1).

For ρ_2 we observe one period-2, one period-6 and one 4-cyclic quasiperiodic attractor lying outside the synchronization manifold M. But there is also a chaotic orbit C constrained to the synchronization manifold M (compare figure 4 and table 1). M is unstable in this case as can be read from Lyapunov exponents $\lambda^s = 0.36$ and $\lambda^\perp = 0.05$ which are both positive (compare table 1). Nevertheless, the orbit C serves as a chaotic attractor for the corresponding synchronized dynamics F^s_ρ constrained to M.

The synchronization manifold M is unstable also for the parameter set ρ_3 (compare figure 5 and table 1). It contains again a chaotic orbit C ($\lambda^s = 0.32,\ \lambda^\perp = 0.008$), which is of course unstable with respect F_ρ, but serves as a chaotic attractor for the corresponding synchronized dynamics F^s_ρ. Outside of M we find a period-4 attractor and a second (2-cyclic) chaotic attractor both arranged symmetrically around M.

There exists a global hyperchaotic attractor for parameter set ρ_4 traversing the unstable synchronization manifold M. Lyapunov exponents are $\lambda^s = 0.149,\ \lambda^\perp = 0.039$ (compare figure 6 and table 1).

Parameter set ρ_5 (compare figure 7 and table 1) demonstrates the instability of the synchronization manifold M for positive couplings $w^{coup} > 0$. There is a hyperchaotic attractor traversing M ($\lambda^s = 0.13,\ \lambda^\perp = 0.047$). A second co-existing 2-cyclic chaotic attractor is found outside of M.

attractor	sync.?	init.cond. (a,b)	λ_1	λ_2	λ^s	$\lambda^\perp$
$\rho_1: \quad \gamma = 0.6, \theta = 4.8, w = -16.0, w^{coup} = -4.0$						
period-2	no	(-3.7,0.1)	-0.116	-0.116	x	x
period-4	no	(-2.804, 0.243)	-0.083	-0.402	x	x
chaotic	yes	(-1.0, -1.0)	x	x	0.353	-0.074
$\rho_2: \quad \gamma = 0.6, \theta = 4.0, w = -16.0, w^{coup} = -3.0$						
period-2	no	(-3.808, -0.076)	-0.036	-0.036	x	x
period-6	no	(-2.804, 0.243)	-0.297	-0.297	x	x
quasiperiodic	no	(-1.263, 1.129)	0.0000	-0.089	x	x
hyperchaotic	yes	(1.0, 1.0)	x	x	0.363	0.056
$\rho_3: \quad \gamma = 0.6, \theta = 4.47, w = -16.0, w^{coup} = -3.0$						
period-4	no	(-9.0, -2.75)	-0.17	-0.17	x	x
chaotic	no	(-5.95, -0.25)	0.108	-0.088	x	x
hyperchaotic	yes	(-1.0,-1.0)	x	x	0.322	0.008
$\rho_4: \quad \gamma = 0.6, \theta = 4.0, w = -16.0, w^{coup} = -2.0$						
hyperchaotic	no	(-0.1, 0.1)	0.149	0.039	x	x
$\rho_5: \quad \gamma = 0.6, \theta = 3.675, w = -16.0, w^{coup} = 2.0$						
chaotic	no	(-2.044, -6.526)	0.119	-0.005	x	x
hyperchaotic	no	(0.577, -8.691)	0.13	0.047	x	x
$\rho_6: \quad \gamma = 0.6, \theta = 4.0, w = -16.0, w^{coup} = 2.0$						
period-4	yes	(1.537, 1.537)	x	x	-1.426	-0.065
quasi	no	(0.281, -9.365)	0.000	-0.655	x	x
hyperchaotic	no	(-6.9, -3.3)	0.084	0.002	x	x

Table 1: Lyapunov exponents for attractors co-existing in a system of two coupled chaotic neurons with parameter sets ρ_1 – ρ_6; compare figures 3 – 8.

Finally, also for positive couplings $w^{coup} > 0$, figure 7 shows a synchronized period-4 attractor in the stable manifold M together with a co-existing 2-cyclic quasiperiodic and a 4-cyclic chaotic attractor (compare table 1).

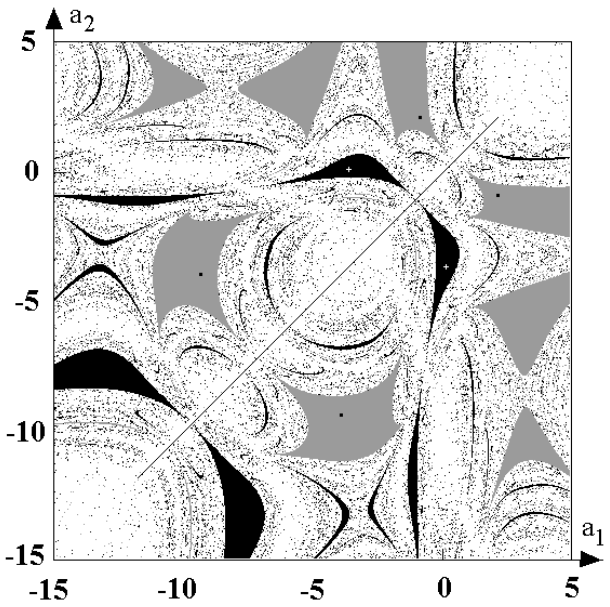

Figure 3: A period-2 (white crosses) and a period-4 attractor (black dots) co-existing with a chaotic attractor in the stable synchronization manifold M together with their basins of attraction (white: chaotic, black: period-2, and gray: period-4 attractor). Parameters: $\gamma = 0.6$, $\theta = 4.8$, $w = -16.0$, $w^{coup} = -4.0$.

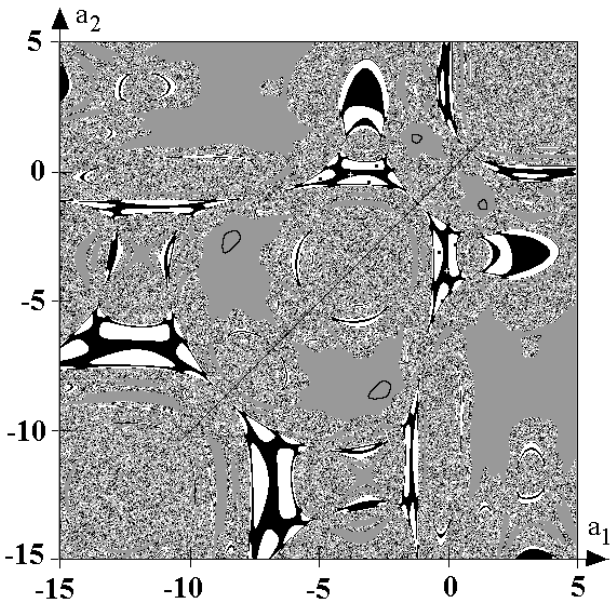

Figure 4: A period-2 (white crosses), a period-6 (black dots) and 4-cyclic quasiperiodic attractor co-existing with a chaotic orbit in the unstable manifold M together with their basins of attraction (white: period-6, black: period-2, and gray: quasiperiodic). Parameters: $\gamma = 0.6$, $\theta = 4.0$, $w = -16.0$, $w^{coup} = -3.0$.

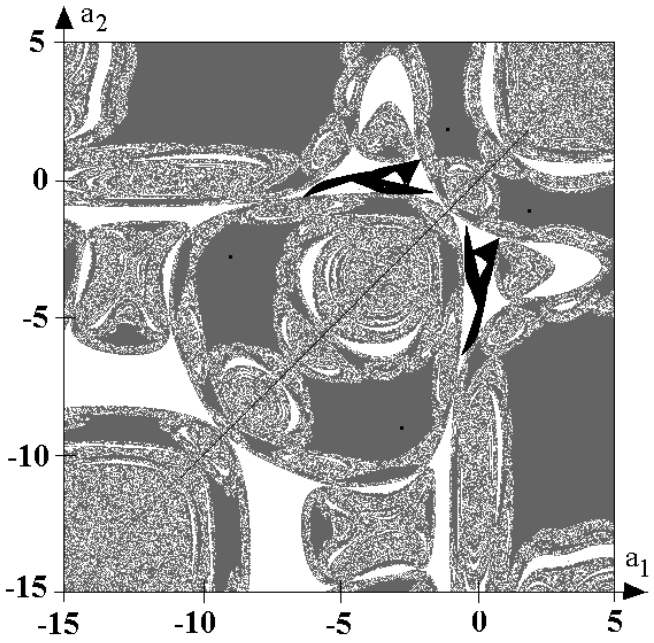

Figure 5: A period-4 (black dots) and a 2-cyclic chaotic attractor co-existing with a chaotic orbit in the unstable manifold M together with their basins of attraction (white: chaotic, and gray: period-4 attractor. Parameters: $\gamma = 0.6$, $\theta = 4.47$, $w = -16.0$, $w^{coup} = -3.0$.

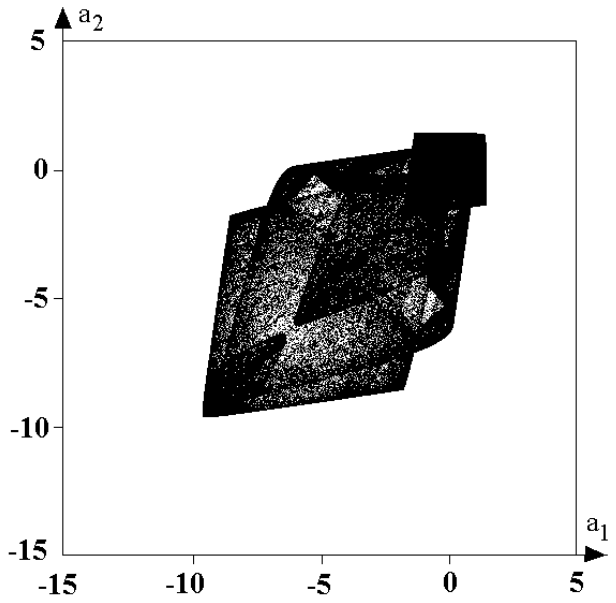

Figure 6: A global hyperchaotic attractor traversing the unstable synchronization manifold M. Parameters : $\gamma = 0.6$, $\theta = 4.0$, $w = -16.0$, $w^{coup} = -2.0$.

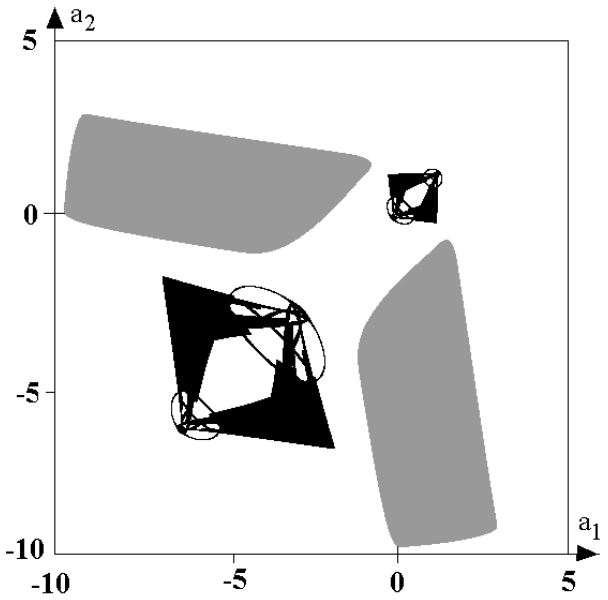

Figure 7: Two co-existing 2-cyclic chaotic attractors (black and gray). The hyperchaotic attractor (black) traverses the unstable synchronization manifold M. Parameters: $\gamma = 0.6$, $\theta = 3.675$, $w = -16.0$, $w^{coup} = 2.0$.

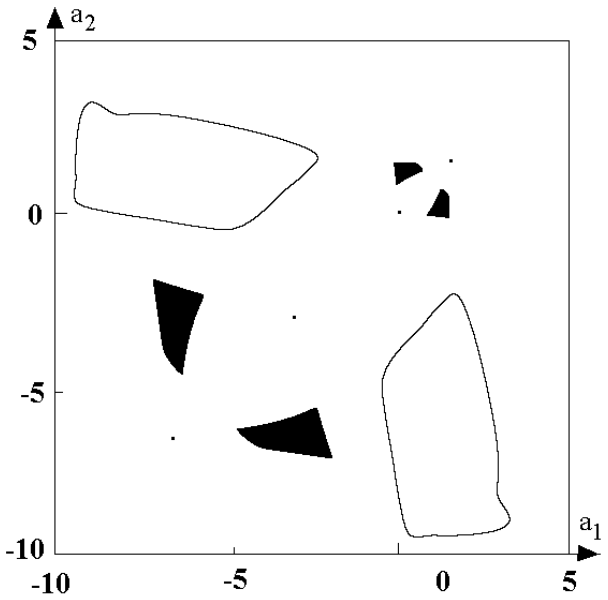

Figure 8: A 2-cyclic quasiperiodic and a 4-cyclic chaotic attractor co-existing with a period-4 orbit in the locally stable synchronization manifold M for parameters $\gamma = 0.6$, $\theta = 4.0$, $w = -16.0$, $w^{coup} = 2.0$.

4 Coupling two non-identical neurons

According to Lemma 1 there exists also a synchronized dynamics for coupled non-identical neurons satisfying condition (5). For instance, keeping w^A and w^{BA} fixed and adjusting w^B and w^{AB} such that they satisfy condition (5) will give again periodic and chaotic dynamics constrained to the synchronization manifold M as can be demonstrated by numerical simulations. As observed for the case of identical neurons with symmetric couplings, there are parameter domains for which M is locally (or even globally) stable, others where the synchronized dynamics is unstable. Cyclic attractors not constrained to M now are of course no longer symmetric to M. Figure 9 displays a bifurcation sequence for the parameter p with $w^B = p$, $w^{AB} = p - w^A + w^{BA}$ and fixed parameters $\gamma = 0.6$, $w^A = -16$, $w^{BA} = -4$, and $\theta = 3$. The whole period-doubling sequence to chaos is contained in M, and the corresponding synchronized dynamics is apparently globally stable over the whole p-interval. For other values of θ this is in general not the case.

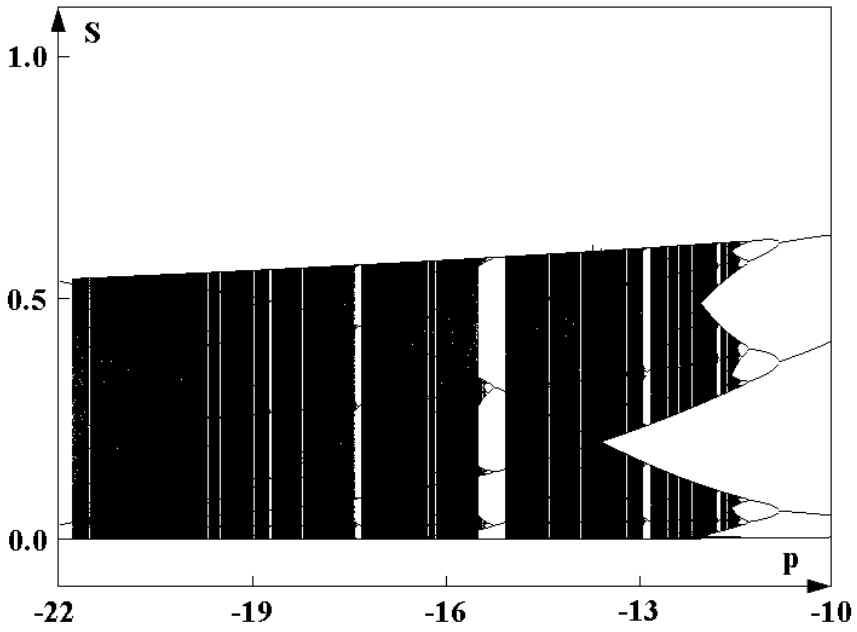

Figure 9: Bifurcation diagram for two coupled non-identical neurons satisfying condition (5). Varied with parameter p are $w^B = p$, $w^{AB} = p - w^A + w^{BA}$; fixed parameters are $\gamma = 0.6$, $w^A = -16$, $w^{BA} = -4$ and $\theta = 3$.

So far synchronized units had identical bias terms (stationary inputs) θ. But, using the symmetry $\sigma(-x) = (1 - \sigma(x))$ of the sigmoide (2), it is easy to prove that (anti-) synchronization of chaotic dynamics can also appear if neurons have different bias terms θ. To give a topologically equivalent dynamics, with respect to coordinate transformations $(a, b) \to (\tilde{a}, \tilde{b}) = (-a, b)$, $(a, -b)$, $(-a, -b)$ bias terms of the units and coupling weights have to be changed in a way described below.

Let the parameters of the coupled system of neurons - satisfying $\gamma = \gamma^A = \gamma^B$ - be given in matrix form as

$$\rho = \begin{pmatrix} \theta^A & w^A & w^{AB} \\ \theta^B & w^B & w^{BA} \end{pmatrix} .$$

We then have the following

Lemma 3 *Consider two chaotic neurons with $\gamma = \gamma^A = \gamma^B$. The dynamics F_ρ of the coupled neurons (3) with respect to the parameter set*

$$\rho = \begin{pmatrix} \theta & w^A & w^{AB} \\ \theta & w^B & w^{BA} \end{pmatrix} .$$

is topologically equivalent to the dynamics $F_{\tilde{\rho}_i}$ with respect to the parameter sets

$$\tilde{\rho}_1 = \begin{pmatrix} \tilde{\theta}^A = -\theta - w^A & \tilde{w}^A = w^A & \tilde{w}^{AB} = -w^{AB} \\ \tilde{\theta}^B = \theta + w^{BA} & \tilde{w}^B = w^B & \tilde{w}^{BA} = -w^{BA} \end{pmatrix} ,$$

$$\tilde{\rho}_2 = \begin{pmatrix} \tilde{\theta}^A = \theta + w^{AB} & \tilde{w}^A = w^A & \tilde{w}^{AB} = -w^{AB} \\ \tilde{\theta}^B = -\theta - w^B & \tilde{w}^B = w^B & \tilde{w}^{BA} = -w^{BA} \end{pmatrix} ,$$

$$\tilde{\rho}_3 = \begin{pmatrix} \tilde{\theta}^A = -\theta - (w^A + w^{AB}) & \tilde{w}^A = w^A & \tilde{w}^{AB} = w^{AB} \\ \tilde{\theta}^B = -\theta - (w^B + w^{BA}) & \tilde{w}^B = w^B & \tilde{w}^{BA} = w^{BA} \end{pmatrix} .$$

Now, suppose parameters ρ satisfy condition (5) of Lemma 1, so that the dynamics F_ρ allows for a synchronized dynamics constrained to M; i.e. $w^- := w^A - w^{BA} = w^B - w^{AB}$ and $w^+ := w^A + w^{AB} = w^B + w^{BA}$. It is obvious, that the synchronous dynamics $F_{\tilde{\rho}_3}$ with respect to parameters $\tilde{\rho}_3$ corresponds again to identical neuron input/bias terms, and it is obtained by the reflection $\tilde{s} = -s$ of the coordinate in M. On the other hand, with respect to parameter sets $\tilde{\rho}_1$ and $\tilde{\rho}_2$ the synchronized dynamics in the new $(\tilde{a}, \tilde{b})$-coordinates corresponds to an anti-synchronized dynamics in the old (a, b) coordinates. We observe that this kind of dynamics is obtained by reversing the coupling strength and changing the bias terms (stationary inputs) correspondingly. For these two cases the bias terms are now no longer identical.

5 Conclusions

In this work it has been shown that in a system of two coupled formal neurons synchronized periodic and chaotic orbits can exist. Depending on parameters, synchronized orbits can be globally stable, locally stable, or unstable. For locally stable synchronized dynamics there do often co-exist periodic, quasiperiodic or even chaotic attractors which correspond to a non-synchronous (but coherent) dynamics. Thus, whether a system ends up in a synchronous behavior asymptotically or not depends crucially on the initial conditions, i.e. on the internal state

of the system, and not only on the external inputs. In this sense the reaction to external signals therefore depends also on the history of the system. This may be related to findings in more biological systems, where there is only a partial synchronization of neurons, even though they share common connections and a common driving signal [3].

Finally we want to point out that the special kind of formal neuron used here may serve as a basic element in larger arrays of coupled neurons. Like in coupled map lattices [13], [19] this type of neural network will show a variety of different dynamical features like partial synchronization, clustering effects and traveling waves of activity. Analysis of these phenomena may help to understand comparable features of biological brains or to setup complex systems with higher information processing capabilities than, for instance, convergent neural networks.

References

[1] Abraham, R. H., Gardini, L. and Mira, C. (1997), *Chaos in Discrete Dynamical Systems*, Springer-Verlag, New York.

[2] Cuomo, K.M. and Oppenheim, A. V. (1993) Circuit implementation of synchronized chaos with applications to communications, *Phys. Rev. Lett.*, **71**, 65–68.

[3] Carroll, T. L. (1995), Synchronization and complex dynamics in pulse-coupled circuit models of neurons, *Biol. Cybern.*, **73**, 553 –559.

[4] Chua, L. O., Kocarev, L. and Eckert, K. (1992), Experimental chaos synchronization in Chua's circuit, *Int. J. Bifurcat. Chaos*, **2**, 705–708.

[5] Dedieu, H., Kennedy, M. P. and Hasler, M. (1993), Chaos shift keying: Modulation and demodulation of a chaotic carrier using self-synchronizing Chua's circuits, *IEEE Trans. Circuits and Systems*, **40**, 732 – 761.

[6] De Sousa Viera, M., Lichtenberg, A. J. and Liebermann, M.A. (1992) Synchronization of regular and chaotic systems, *Phys. Rev. A*, **46**, 7359–7362.

[7] Ding, M. and Ott, E. (1994), Enhancing synchronism of chaotic systems, *Phys. Rev. E*, **49**, R945–R449.

[8] Eckhorn, R., Bauer, R., Jordan, W., Brosch, M., Kruse, W., Munk, M. and Reitboeck H. J. (1988) Coherent oscillations: a mechanism for feature linking in the visual cortex. *Biol. Cybern.*, **60**, 121-130.

[9] Engel, A. K., Roelfsema, P. R, Fries, P., Brecht, M. and Singer, W. (1997) Binding and response selection in the temporal domain - a new paradigm for neurobiological research? *Theory in Biosciences*, **116**, 241-266.

[10] Hansel, D. and Sompolinsky H. (1992) Synchronization and computation in a chaotic neural network *Phys. Rev. Lett.*, **68**, 718–721.

[11] Heagy, J. F., Carroll, T. L. and Pecora, L. M., (1994), Synchronous chaos in coupled oscillator systems, *Phys. Rev. E*, **50**, 1874–1885.

[12] John, J. K. and Amritkar, R. E. (1994) Synchronization by feedback and adaptive control. *Int. J. Bifurcat. Chaos*, **4**, 1687–1696.

[13] Kaneko, K. (1994) Relevance of dynamical clustering to biological networks, *Physica D*, **75**, 55–73.

[14] Kapitaniak, T. and Steeb, W.-H. (1991) Transition to hyperchaos in coupled generalized van der Pol's equations. *Phys. Lett. A*, **152**, 33-36.

[15] Kittel, A., Parisi, J. and Pyragas, K. (1998), Generalized synchronization of chaos in electronic circuit experiments, *Physica D*, **112**, 459–471.

[16] Kocarev, L., Halle, K. S., Eckert, K., Chua, L. O. and Parlitz, U. (1992), Experimental demonstration of secure communication via chaotic synchronization, *Int. J. Bifurcat. Chaos*, **2**, 709–713.

[17] Kocarev, L., Shang, A. and Chua, L. O. (1993) A unified method of control and synchronization of chaos, *Int. J. Bifurcat. Chaos*, **3**, 479–483.

[18] Kocarev, L. and Parlitz, U. (1995), General approach for chaotic synchronization with applications to communication *Phys. Rev. Lett.*, **74**, 5028–5031.

[19] Nozawa, H. (1994), Solution of the optimization problem using neural network model as global coupled map, in: Yamaguti, M. (ed.) *Toward the harnessing of Chaos*, Amsterdam: Elsevier.

[20] Parlitz, U., Chua, L. O., Kocarev, L., Halle, K. S. and Shang, A. (1992) Transmission of digital signals by chaotic synchronization, *Int. J. Bifurcat. Chaos*, **2**, 973–977.

[21] Pasemann, F. (1997) A simple chaotic neuron *Physica D*, **104**, 205–211.

[22] Pasemann, F. (1998), Structure and dynamics of recurrent neuromodules, *Theory in Biosciences*, **117**, 1–17.

[23] Pecora, L. M. and Carroll, T. L. (1990), Synchronization in chaotic systems, *Phys. Rev. Lett.*, **64**, 821–823.

[24] Pecora, L. M. and Carroll, T. L. (1991), Driving systems with chaotic signals, *Phys. Rev.*, **A44**, 2374 –2383.

[25] Pecora, L. M., Heagy, J. and Carroll, T. L. (1994), Synchronization and desynchronization in pulse-coupled relaxation oscillators, *Phys. Lett. A*, **186**, 225–229.

[26] Pecora, L. M., Carroll, T. L., Johnson, G. and Mar, D. (1997), Volume-preserving and volume-expanding synchronized chaotic systems *Phys. Rev. E*, **56**, 5090–5100.

[27] Pikovsky, A. S. (1984), On the interaction of strange attractors, *Z. Phys. B*, **55**, 149–154.

[28] Rössler, O. (1979) An equation for hyperchaos. *Phys. Lett. A*, **71**, 155-157.

[29] Schweizer, J., Kennedy, M. P., Hasler, M. and Dedieu, H. (1995) Synchronization theorem for a chaotic system. *Int. J. Bifurcat. Chaos*, **5**, 297–302.

[30] Singer, W. (1994) Time as coding space in neocortical processing. In: Buzsáki, G.; Llinás, R.; Singer, W.; Berthoz, A. and Christen, Y. (eds.) *Temporal Coding in the Brain*. Springer, Berlin. pp. 51-80.

[31] Tesi, A., de Angeli, A. and Genesio, R. (1994) On system decomposition for synchronized chaos *Int. J. Bifurcat. Chaos*, **4**, 1675–1686.

[32] Wennekers, T. and Pasemann, F. (1996), Synchronous chaos in high-dimensional modular neural networks. *Int. J. Bifurcat. Chaos*, **6**, 2055-2067.